Intense-laser-field-enhanced ionization of two-electron molecules: Role of ionic states as doorway states

doi: 10.1103/PhysRevA.62.031401

PHYSICAL REVIEW A, VOLUME 62, 031401(R)

Intense-laser-field-enhanced ionization of two-electron molecules: Role of ionic states as doorway states

Isao Kawata,[1] Hirohiko Kono,[1] Yuichi Fujimura,[1] and André D. Bandrauk[2]
[1]*Department of Chemistry, Graduate School of Science, Tohoku University, Sendai 980-8578, Japan*
[2]*Laboratoire de Chimie Théorique, Faculté des Sciences, Université de Sherbrooke, Sherbrooke, Quebec, Canada J1K2R1*
(Received 27 March 2000; published 3 August 2000)

We investigate the mechanism of enhanced ionization in two-electron molecules by solving exactly the time-dependent Schrödinger equation for a one-dimensional H_2 in an ultrashort, intense ($I \geqslant 10^{14}$ W/cm^2) laser pulse ($\lambda = 1064$ nm). Enhanced ionization in two-electron systems differs from that in one-electron systems in that the excited ionic state H^-H^+ regarded as the dominant doorway state to ionization crosses the covalent ground state HH in field-following time-dependent adiabatic energy. An analytic expression for the crossing condition obtained in terms of the lowest three states agrees with the numerical results. The gap at the avoided crossing decreases the initial covalent component and promotes electron transfer to H^-H^+. As the internuclear distance R decreases, the population of the H^-H^+ created increases, whereas the ionization rate from a H^-H^+ decreases owing to the stronger attraction by the distant nucleus. As a result, the rate has a peak at $R \approx 6$ a.u., where most adiabatic states avoid each other with considerable gaps.

PACS number(s): 42.50.Hz, 32.80.Rm

The investigation of the interaction of atoms with ultrashort intense laser pulses in the nonlinear multiphoton excitation regime has led to the discovery of different nonperturbative phenomena such as above-threshold ionization and tunneling ionization [1]. In the low-frequency regime, such nonperturbative phenomena can be understood in terms of quasistatic plasma physics models [2,3]. For the case of molecules, a different nonperturbative phenomenon, charge resonance-enhanced ionization, has been discovered. Recent exact numerical simulations of ionization in one-electron systems such as H_2^+ [4–6], H_3^{+2}, and others [7,8] have shown that the ionization rate takes a maximum at critical internuclear distances R_c and far exceeds those of the neutral fragments. Enhanced ionization has been observed in recent experiments [9]. The extra degree of freedom arising from nuclear motion necessitates the use of alternative concepts such as avoided potential crossings in a laser field. Field-induced nonadiabatic transitions through crossing points, as well as nuclear-motion induced ones, are essential to describing the ionization dynamics [10–12].

The system H_2^+ is regarded as a prototype of odd-electron molecules. The electronic dynamics in H_2^+ prior to ionization is determined by the radiative coupling between the highest occupied molecular orbital (HOMO) and the lowest unoccupied molecular orbital (LUMO), $1\sigma_g$ and $1\sigma_u$. The transition moment between them increases with internuclear distance R as $R/2$, which has been originally emphasized by Mulliken as a charge resonance transition between a bonding and a corresponding antibonding molecular orbital (MO) [13]. The strong radiative coupling changes the energies of $1\sigma_g$ and $1\sigma_u$ up to the ''field-following'' HOMO and LUMO energies at the maximum field amplitude $\mathcal{E}_0$, $E_{\mp}(R) \approx I_p \mp \mathcal{E}_0 R/2$ [11], where I_p is the ionization potential of H. The instantaneous electrostatic potential for the electron has a descending and an ascending potential well that yield the adiabatic energies E_- and E_+, respectively. There exist barriers between the two wells and outside the descending well. On the assumption that, at R_c, $E_+(R)$ is equal to the tops of the two barriers, one can obtain analytic expressions for R_c; for H_2^+, $R_c \approx 4/I_p$ [4,5] whereas for H_3^{+2}, $R_c \approx 5/I_p$ [7]. These R_c are consistent with the numerical simulations of ionization, which indicates that the ionization proceeds via the field-following LUMO state nonadiabatically created from the HOMO state. This mechanism has been directly proved by monitoring the populations of field-following adiabatic states [11]. The enhanced ionization in odd-electron molecules is due to the single-electron transfer to the ascending well.

Maxima in the ionization rate have been found for two-electron model systems such as H_2 and H_4^{+2} in one-dimensional (1D) space. The existence of similar R_c's as the one-electron systems [7] indicates that enhanced ionization is a universal phenomenon. We, however, expect that the mechanism of the enhanced ionization in even-electron molecules differs from that in the odd-electron cases: in even-electron cases, excited electron transfer ionic states can cross the covalent ground state in field-following adiabatic energy. The roles of ionic and covalent states in ionization should be clarified. We reveal the efficiency of electron transfer from the covalent state to the lowering ionic state as a function of R and the origin of the R dependence in the ionization probability. In this Rapid Communication, we investigate the mechanism of the enhanced ionization in H_2 as a prototype of even-electron molecules.

We begin with a simple MO picture to discuss the crossing of the covalent and ionic states. For H_2, one must consider at least the lowest three electronic states, $1\sigma_g^2(X^1\Sigma_g^+)$, $1\sigma_g 1\sigma_u(B^1\Sigma_u^+)$, and $1\sigma_u^2(E,F^1\Sigma_g^+)$. The asymptotic atomic dissociation products ϕ_1, ϕ_2, and ϕ_3 for these states are, in the MO approximation, expressed as [14]

$$\phi_1(1,2) = [a(1)a(2) + b(1)b(2) + a(1)b(2) + b(1)a(2)]/2, \quad (1)$$

$$\phi_2(1,2) = [a(1)a(2) - b(1)b(2)]/\sqrt{2}, \quad (2)$$

$$\phi_3(1,2)=[a(1)a(2)+b(1)b(2)-a(1)b(2) -b(1)a(2)]/2, \quad (3)$$

where a and b denote the $1s$-like atomic orbitals on protons a and b, respectively, and 1 and 2 represent the coordinates of the two electrons. Both ground ϕ_1 and second excited ϕ_3 states are linear combinations of *ionic* (aa,bb) and *covalent* (ab) configurations, whereas the first excited state ϕ_2 is purely ionic.

The transition moments between the states are given by $\langle\phi_1|z|\phi_2\rangle=\langle\phi_2|z|\phi_3\rangle=R/\sqrt{2}$ [13]. The three states (1)–(3) are thus coupled by the same radiative matrix element $\mathcal{E}_0R/\sqrt{2}$. Diagonalizing the 3×3 energy matrix yields the following adiabatic energies and states at $\mathcal{E}_0$:

$$E_0=0, \quad \phi_0=[a(1)b(2)+b(1)a(2)]/\sqrt{2}, \quad (4)$$

$$E_+=\mathcal{E}_0R, \quad \phi_+=b(1)b(2), \quad (5)$$

$$E_-=-\mathcal{E}_0R, \quad \phi_-=a(1)a(2). \quad (6)$$

The result is exact provided that $\mathcal{E}_0R$ are much larger than the zero-field energy separations between ϕ_1, ϕ_2, and ϕ_3. The ground state (6) is the ionic state $H_a^-H_b^+$ whose energy agrees with the electrostatic energy of a charge displaced through the distance R by a field $\mathcal{E}_0$.

We add next the Coulomb potentials to the above treatment [15]. Consider the general charge transfer $A^{+q}A^{+q} \rightarrow A^{+q-1}A^{+q+1}$. The initial total energy is $E_{q,q}(R)=-2I_p(q)+q^2/R$, where $I_p(q)$ is the ionization potential of A^{+q} and q^2/R is the ion-ion repulsion. Throughout this Rapid Communication, atomic units are used unless otherwise noted. The final energy of the charge transfer state in the field is $E_{q-1,q+1}(R)=-I_p(q-1)-I_p(q)+(q+1)(q-1)/R-\mathcal{E}_0R$. The difference, $E_{q-1,q+1}-E_{q,q}$, is $\Delta E=\Delta I_p-1/R-\mathcal{E}_0R$, where $\Delta I_p=I_p(q)-I_p(q-1)$. The field strength required for the expected crossing of the covalent $A^{+q}A^{+q}$ and ionic $A^{+q-1}A^{+q+1}$ states, $\mathcal{E}_c$, is determined from $\Delta E=0$ as $\mathcal{E}_c=(\Delta I_p-1/R)/R$. Using the 1D H_2 model described below, we show next that the ionic state indeed becomes the ground state for $\mathcal{E}_0\geq\mathcal{E}_c$ and that the ionic state created determines the ionization process.

We employ a 1D H_2 model [7(a)] in which the two electrons move only along the molecular axis and R is treated as a parameter. The coordinates of the two electrons are denoted by z_1 and z_2, respectively. The potential of the unperturbed Hamiltonian $H_0(z_1,z_2)$ has two minima at the *covalent* (C) configurations around $z_1=-z_2=\pm R/2$ and two saddle points at the *ionic* (I) configurations around $z_1=z_2=\pm R/2$. See, for the corresponding wave functions, Eqs. (4)–(6). In the high intensity and low-frequency regime, the molecule ionizes mainly when it is parallel to the polarization of the field $\mathcal{E}(t)$ [8(b)]. Thus we employ the form $V_{\mathcal{E}}(t)=(z_1+z_2)\mathcal{E}(t)$ as the effective dipole interaction. The field $\mathcal{E}(t)$ is assumed to be $f(t)\sin(\omega t)$, where ω is the frequency and the envelope $f(t)$ is linearly ramped with time t so that after five cycles $f(t)$ attains its maximum $\mathcal{E}_0$. The field parameters are as follows: $\mathcal{E}_0=0.12$ a.u. ($I=5\times10^{14}$ W/cm^2) and $\omega=0.0428$ a.u. ($\lambda=1064$ nm). The time-dependent Schrödinger equation for the system is solved by using the method described in Ref. [11].

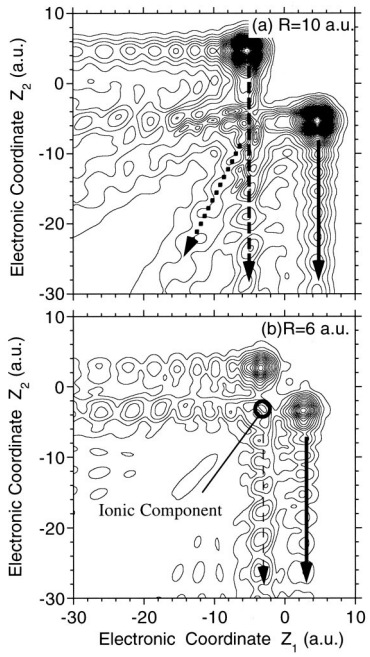

FIG. 1. Snapshots of the electronic wave packet $|\Psi(z_1,z_2)|$ at $t=642$ a.u. for (a) $R=10$ a.u. and (b) 6 a.u. $\mathcal{E}(t)=0.62$ a.u. ($\mathcal{E}_0=0.12$ a.u.), and $\omega=0.0428$ a.u. The intervals of the contour lines are constant. The bold solid line denotes ionization from the descending well ($z_2=-R/2$); the bold broken line in (a) denotes ionization from the ascending well ($z_2=R/2$); the dotted line in (a) denotes simultaneous two-electron ionization; the ionization from the ionic component created (around the bold circle) is indicated by the thin broken line in (b).

We first outline features of the intense field ionization processes at $R=6$ and 10 a.u. Shown in Fig. 1 are the two snapshots $|\Psi(z_1,z_2)|$ at $t=4\frac{3}{8}$ cycle. The initial state is the exact ground state ϕ_1 of H_0 [Eq. (1) in the MO approximation]. The singlet state has the exchange symmetry $\Psi(z_1,z_2)=\Psi(z_2,z_1)$ [14]. As shown in Fig. 1(a), for $R=10$ a.u., ionization starts from the C configurations. An electron near the descending well where $z\mathcal{E}(t)<0$ [the left nucleus when $\mathcal{E}(t)>0$] is ejected as indicated by the solid line with an arrow [referred to as covalent (C) type]. Another C-type ionization that starts from the ascending well is indicated by the broken line; in this process, the electron ejected from the ascending well penetrates through the descending one without colliding with the other electron. The collision between the electrons leads to the simultaneous two-electron ionization indicated by the dotted line. The electron ejected from the ascending well gains kinetic energy of $\sim R\mathcal{E}_0$ by the time it collides with the electron in the descending well. For $R=10$ a.u., $R\mathcal{E}_0\approx1$ a.u. is larger than $I_p(1\text{D H})=0.67$ a.u.

For $R=6$ a.u., as shown in Fig. 1(b), an ionic (I) component is created near the descending well because of the laser-induced electron transfer from the ascending well. As indicated by the thin broken line, an electron is ejected from the I configuration [referred to as ionic (I) type]. The importance of the I configuration is obvious from the fact that the ion-

TABLE I. Ionic components in eigenfunctions $|\phi_l\rangle$ of the 1D H_2 Hamiltonian, H_0. The gerade and ungerade components are denoted by subscripts g and u, respectively.

	l	1	2	3	4	5	6	7
$R=4.25$ a.u.	$\lvert\langle\Psi^I_{g,u}\rvert\phi_l\rangle\rvert^2$	0.45_g	0.71_u	0.23_g	0.27_g	0.09_u	0.01_g	0.08_u
$R=6$ a.u.	$\lvert\langle\Psi^I_{g,u}\rvert\phi_l\rangle\rvert^2$	0.16_g	0.49_u	0.38_g	0.40_g	0.42_u	0.06_u	0.02_g
$R=10$ a.u.	$\lvert\langle\Psi^I_{g,u}\rvert\phi_l\rangle\rvert^2$	0.01_g	0.03_u	0.03_g	0.79_g	0.79_u	0.15_u	0.15_g

ization current from the I configuration is four times as large as that for the C type denoted by the solid line. The I configuration has a very low ionization potential as I_p ($1D\,H^-$) $=0.06$ a.u. and is regarded as a doorway state to ionization. To quantify the I component, we define the localized I configurations $\Psi_{H^+H^-}$ and $\Psi_{H^-H^+}$ as the exact ground state H^- atoms at $z=\pm R/2$. The $\Psi_{H^+H^-}$ and $\Psi_{H^-H^+}$ correspond to the ''field'' MO's Eqs. (5) and (6), respectively. At $R\approx 6$ a.u., the I component created becomes large as $|\langle\Psi_B|\Psi_{H^-H^+}\rangle|^2\approx 0.2$ in the fourth cycle (for $R=10$ a.u., $|\langle\Psi_B|\Psi_{H^-H^+}\rangle|^2\approx 0.02$), where Ψ_B is the *normalized* packet for the projection of the exact $\Psi(t)$ onto the bound eigenstates of H_0.

The radiative interaction $V_{\mathcal{E}}(t)$ can couple two eigenstates of *gerade* and *ungerade* inversion symmetry. The transition moment between the 1D exact ground ϕ_1 and first excited ϕ_2 states increases as $R/\sqrt{2}$ up to $R\approx 3$ a.u. and converges to $\sqrt{2}\times$(atomic value), which is consistent with accurate calculations for the three-dimensional (3D) H_2 [16]. The linear increase with R typical of the simple MO approximation [13] indicates that in the small R (<6 a.u.) region the exact ϕ_1 includes considerable gerade I component Ψ^I_g as in Eqs. (1) and (3) and ϕ_2 includes the ungerade I component Ψ^I_u, Eq. (2); i.e., $\Psi^I_{g,u}\equiv c_\pm(\Psi_{H^+H^-}\pm\Psi_{H^-H^+})$, where $c_\pm$ are normalization constants. As shown in Table I, as R increases, $\Psi^I_{g,u}$ are distributed among higher states. Since $\langle\Psi^I_u|z|\Psi^I_g\rangle$ is as large as R [13], the I components involved dominate transition moments: as shown by Eqs. (4)–(6), the structures $\Psi_{H^+H^-}$ and $\Psi_{H^-H^+}$, which are linear combinations of Ψ^I_g and Ψ^I_u, are easily formed in an intense field whenever Ψ^I_g or Ψ^I_u is involved in the initial state.

Comparing the two panels in Fig. 1, one notices that the population remaining in the bound states of H_0 is smaller for $R=6$ a.u. than for $R=10$ a.u. (the ionization rate at $R=6$ a.u. is five times as large as that at $R=10$ a.u.). As reported in a previous paper [7(a)], the ionization rate has a peak (or peaks) around $R=5-6$ a.u. To fully understand the mechanism of the enhanced ionization and the role of ionic configurations, we map $\Psi(t)$ onto adiabatic states defined as eigenfunctions $|n\rangle$ of the ''instantaneous'' Hamiltonian $H(t)=H_0+V_{\mathcal{E}}(t)$ [11]. For the diagonalization of $H(t)$, the lowest seven eigenstates of H_0, $\{\phi_l\}$, are used. Equations (1)–(3) are approximate forms for the lowest three ϕ_l ($l=1-3$).

The calculated adiabatic energies $E_n(t)$ for $|n\rangle$ at $R=10$, 6, and 4.25 a.u. are plotted in Fig. 2. The field is the same as in Fig. 1. The $|1\rangle$ represents the ground state near zero field as Eq. (1); $|1'\rangle$, $|2\rangle$, and $|3\rangle$ represent the lowest three adiabatic states near the field maxima. The overall level dynamics is governed by transition probabilities at crossing points. The gap at an avoided crossing between adiabatic states n and m is twice as large as the diabatic coupling $v_{\overline{nm}}=\langle\overline{n}|z|\overline{m}\rangle\mathcal{E}(t)$ at the crossing, where $\overline{n}$ and $\overline{m}$ represent the two states in the corresponding diabatic representation. The nonadiabatic n-m transition probability P_{nm} for the general two-level crossing problem is given by the Landau-Zener formula $\exp[-2\pi v^2_{\overline{nm}}/|d\Delta E_{\overline{nm}}/dt|]$, where $\Delta E_{ij}=E_i-E_j$ [17]; the adiabatic one is $P_{\overline{nm}}\equiv 1-P_{nm}$. As the $\overline{n}$-$\overline{m}$ spatial overlap or the $\Psi^I_{g,u}$ involved decreases, $v_{\overline{nm}}$ and $P_{\overline{nm}}$ decrease.

In the large R (≈ 10 a.u.) region as in Fig. 2(a), the initial state $|1\rangle$ is mainly covalent, $|1'\rangle$ is ionic, and $|2\rangle$ is covalent. The state $|1'\rangle$, whose energy changes on a large scale as $\sim R\mathcal{E}(t)$, becomes the ground state when $|\mathcal{E}(t)|\geqslant 0.05$. This crossing agrees with the prediction $\mathcal{E}_c=0.051$ a.u. ($\Delta I_p=0.61$ a.u.). Population analysis, however, shows that $|1'\rangle$ is little populated ($|\langle 1'|\Psi_B\rangle|^2\approx 0.01$ at $t\approx 700$ a.u.): $|1\rangle$ is only weakly coupled with the ionic one $|1'\rangle$ because of the negligible avoided crossing between them. The distance of $R=10$ a.u. is too large for an electron to adiabatically jump to the other nucleus. As a result, the main path follows the covalent one $|1\rangle\rightarrow|2\rangle\rightarrow|1\rangle$. Near the field maximum, the population of $|2\rangle$ decreases owing to the C-type and simultaneous two-electron ionization processes as shown in Fig. 1(a).

In the intermediate region ($R\approx 6$ a.u.) where enhanced ionization occurs, all the lowest five states of H_0 have an ionic character. See Table I. Whenever adiabatic energies are close, as shown in Fig. 2(b), avoided crossings through the ionic character exist. The dominant character of $|1\rangle$ is cova-

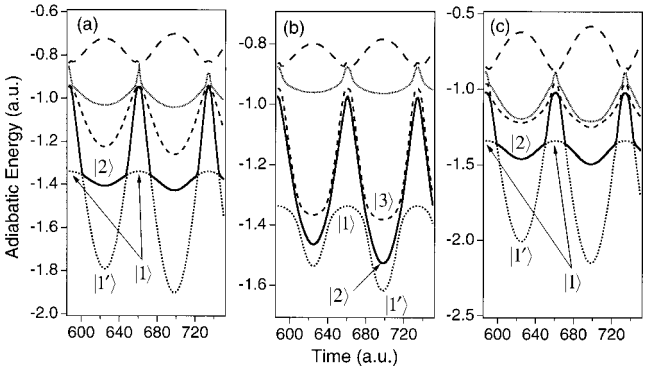

FIG. 2. The energies $\{E_n\}$ of the lowest five adiabatic states as functions of time t: (a) $R=10$, (b) 6, and (c) 4.25 a.u. The laser field is the same as used in Fig. 1. Five line species are used to denote $\{E_n\}$ for $n=1-5$; e.g., the solid line denotes E_2. $|1\rangle$ represents the ground state near zero field; $|1'\rangle$, $|2\rangle$, and $|3\rangle$ represent the lowest three adiabatic states near the field maxima. As the gap at an avoided crossing is larger, the transition becomes adiabatic. In (b), maximum avoided crossing is observed.

lent; $|1'\rangle$ is a Rydberg-like spatially ''diffuse'' state (<20% ionic) originating from the third and higher excited states of 1D H, $|2\rangle$ is ionic (75% at $t \approx 700$ a.u.), and $|3\rangle$ is covalent. From population analysis, the transition probabilities for the crossing at $t=680$ a.u. are as follows: $P(1\rightarrow 1'):P(1\rightarrow 2):P(1\rightarrow 3)=0:1:2$. Compare the *I* and *C* components in Fig. 1(b). Reducing the three-level crossing to two two-level problems $1\rightarrow 1'$ and $1\rightarrow 2$, $P(1\rightarrow 1')/P(1\rightarrow 2)$ can be estimated by $\bar{P}_{11'}/\bar{P}_{12} \approx v_{11'}^2 (d\Delta E_{12}/dt)/v_{12}^2 (d\Delta E_{11'}/dt)$. The coupling v_{12} is six times as large as $v_{11'}$ because of the larger *I* component in $|2\rangle$. Energy matching is also unfavorable to the channel $1\rightarrow 1'$; i.e., $d\Delta E_{11'}/dt > d\Delta E_{12}/dt$. The adiabatic channel to the diffuse state $1\rightarrow 1'$ is hence closed.

Energy matching and spatial overlap are most favorable to the covalent channel $1\rightarrow 3$. The ionic state $|2\rangle$, however, intrudes into the channel as shown in Fig. 2(b). The intervention of the ionic state is in accord with the ionic and covalent crossing condition $|\mathcal{E}(t)|>\mathcal{E}_c=0.074$ a.u. at $R=6$ a.u. The resultant avoided crossing reduces the $1\rightarrow 3$ transition probability and the residual population goes into $|2\rangle$: the avoided crossing creates an *I* component (H^-H^+) while reducing the *C* component. It should be pointed out that maximum avoided crossing occurs at $R=6$ a.u. The coexistence of the channels $|1\rangle\rightarrow$ionic$|2\rangle$ and $|1\rangle\rightarrow$covalent$|3\rangle$ is a result of the efficient electron transfer from the initial covalent state by the maximum avoided crossing. For the present 10th half cycle, the ionization probability from $|2\rangle$ is nearly unity (owing to *I* type). The population of $|3\rangle$ is reduced to $\frac{1}{2}$ (*C* type). The ionization probability from a pure covalent state is much smaller than the ionization probability from H^-H^+ and is nearly independent of *R* (The *C*-type ionization can be explained as the ionization of H). The enhanced ionization is hence determined by the population of the main doorway state to ionization, H^-H^+, and the ionization probability from H^-H^+.

For $R=4.25$ a.u., $\Psi(t)$ follows the path $|1\rangle\rightarrow|2\rangle\rightarrow|1\rangle$ in Fig. 2(c). The diabatic path alternates between $|1\rangle$ (45% ionic) and the more ionic state $|2\rangle$ (75% at $\mathcal{E}(t)\approx\mathcal{E}_0$). The states $|1\rangle$ and $|2\rangle$ correspond to Eqs. (1) and (6). Although $|1\rangle$ crosses a diffuse state $|1'\rangle$ in energy when $|\mathcal{E}(t)| \approx 0.05$ a.u., transitions $1\rightarrow 1'$ hardly occur due to the negligible spatial overlap ($v_{11'}\approx 3\times 10^{-4}$). Near the field maximum, the population of $|2\rangle$ decreases due to *I*-type ionization: $|2\rangle$ is identified as the doorway state to ionization. Although the H^-H^+ involved is larger at $R\approx 4$ a.u. than at $R\approx 6$ a.u. ($|\langle\Psi_B|\Psi_{H^-H^+}\rangle|^2 \leq 0.4$ for $R=6$ a.u.), the ionization rate is a little larger at $R\approx 6$ a.u. than at $R\approx 4$ a.u. As *R* decreases, the ionization rate decreases because the two electrons in H^-H^+ are more strongly attracted by the distant nucleus. For the seventh half cycle [$f(t)\approx 0.078$ a.u.], the ionization probability from H^-H^+ decreases as 1, 0.55, and 0.34 at $R=6$, 4.25, and 3 a.u., respectively. The overall ionization is therefore enhanced around $R=6$ a.u.

In conclusion, the localized ionic configuration in the descending well is the main doorway state to ionization. In the large $R(\approx 10$ a.u.) region, the dynamics follows the covalent path. As *R* decreases, the population of H^-H^+ increases, whereas the ionization rate from a pure H^-H^+ decreases. As a result, the rate has a peak at the critical distance $R_c \approx 6$ a.u., where most adiabatic states avoid each other with considerable gaps. The gap at the avoided crossing between the covalent and ionic states decreases the initial covalent component and promotes the electron transfer from the ascending well to H^-H^+. What correlates with R_c is not just the crossing but the extensive avoided crossing (i.e., how extensively the ionic character is distributed among states). More efficient electron transfer indicates the stronger attraction by the distant nucleus, which decreases the ionization rate from a pure H^-H^+.

The diffuse (Rydberg-like) state is not considered in the three state model, Eqs. (4)–(6), as it plays no role in the dynamics owing to negligible coupling with the dominant covalent and ionic states, Eqs. (4) and (6). The main coupling via the field and the electron correlation is always between the two essential states, the covalent and ionic ones. Thus the resultant dynamics in intense fields can be elucidated by the three-state model. This simple model furthermore supports the electrostatic consideration of field-induced charge-asymmetric dissociation of I_2 by Gibson *et al.* [18].

A.D.B. received support from The Ministry of Education, Science and Culture of Japan while this work was conducted.

[1] M. Gavrila, *Atoms in Intense Fields* (Academic Press, New York, 1992).

[2] P. B. Corkum *et al.*, in *Atoms in Intense Fields* (Ref. [1]), p. 109; Phys. Rev. Lett. **62**, 1259 (1989).

[3] P. B. Corkum, Phys. Rev. Lett. **71**, 1994 (1993).

[4] T. Zuo and A. D. Bandrauk, Phys. Rev. A **48**, 3837 (1993); **52**, R2511 (1995); **54**, 3254 (1996).

[5] S. Chelkowski and A. D. Bandrauk, J. Phys. B **28**, L723 (1995).

[6] T. Seidemann *et al.*, Phys. Rev. Lett. **75**, 2819 (1995).

[7] (a) H. Yu, T. Zuo, and A. D. Bandrauk, Phys. Rev. A **54**, 3290 (1996); (b) A. D. Bandrauk, Comments At. Mol. Phys. D **1**, 97 (1999).

[8] (a) H. Yu *et al.*, J. Phys. B **31**, 1533 (1998); (b) A. D. Bandrauk and J. Ruel, Phys. Rev. A **59**, 2153 (1999).

[9] A. Hishikawa *et al.*, Phys. Rev. Lett. **83**, 1127 (1999).

[10] A. D. Bandrauk, *Molecules in Intense Laser Fields* (M. Dekker, New York, 1994), Chap. 1–3.

[11] I. Kawata *et al.*, J. Chem. Phys. **110**, 11152 (1999); Chem. Phys. Lett. **289**, 546 (1998).

[12] P. Dietrich *et al.*, Phys. Rev. Lett. **77**, 4150 (1996).

[13] R. S. Mulliken, J. Chem. Phys. **7**, 20 (1939).

[14] J. C. Slater, *Quantum Theory of Molecules and Solids* (McGraw-Hill, New York, 1963), Vol. I.

[15] A. D. Bandrauk, in *The Physics of Electronic and Atomic Collisions*, edited by Y. Itikawa *et al.* AIP Conf. Proc. No. 500 (AIP, New York, 1999), p. 102.

[16] L. Wolniewicz, J. Chem. Phys. **51**, 5002 (1969).

[17] H. Nakamura and C. Zhu, Comments At. Mol. Phys. **32**, 249 (1996).

[18] G. N. Gibson *et al.*, Phys. Rev. A **58**, 4723 (1998).